

DESIGN, SYNTHESIS AND BIOLOGICAL EVALUATION OF TRIAZINE-4-THIAZOLIDINONE HYBRID MOLECULES AS MODULATOR OF BREAST CANCERRabin Debnath^{*1}, Deepak Singh Bisht², Saurabh Saklani², Suman Yadav² and Poonam Rishishwar³¹Assistant Professor, NEPEDS College of Pharmaceutical Sciences Gandhinagar, Sonapur, Tetelia, Kamrup (M), Assam-782403.²Assistant Professor, Faculty of Pharmacy, Maharaja Agrasen Himalayan Garhwal University, Pokhra, Pauri Garhwal-246169, Uttarakhand (India).³Head and Professor, Faculty of Pharmacy, Maharaja Agrasen Himalayan Garhwal University, Pokhra, Pauri Garhwal-246169, Uttarakhand (India).***Corresponding Author: Rabin Debnath**

Assistant Professor, NEPEDS College of Pharmaceutical Sciences Gandhinagar, Sonapur, Tetelia, Kamrup (M), Assam-782403.

Article Received on 14/11/2024

Article Revised on 04/12/2024

Article Accepted on 24/12/2024

ABSTRACT

Background: Breast cancer, characterized by uncontrolled cell proliferation and the ability to invade other tissues, remains a leading cause of cancer-related morbidity and mortality worldwide. The multifactorial nature of breast cancer involves genetic mutations, hormonal influences, and complex cellular signaling pathways. **Objective:** We aim to design novel compounds based on reported active pharmacophoric features and validate them through molecular modeling. These designed compounds will then be synthesized and characterized. Finally performed a biological evaluation of the synthesized compounds to assess their efficacy. **Method:** Firstly thirty compounds were designed based on literature survey out of these compounds twelve compounds were found to be most potent based on the docking studies and these twelve new derivatives (RD 01-12) were synthesized and subjected to *in silico*, *in vitro* (EGFR assay), and ADMET profiling to identify the most potent compound. **Result:** Compound RD-09 emerged as the most potent, with an IC_{50} value of $1.21 \pm 0.03 \mu M$, confirmed by docking studies it possesses a docking score of -7.302 against EGFR receptor. These compounds were further characterized using IR, NMR, and mass spectrometry. **Conclusion:** In this study, twelve triazine-4-thiazolidinone derivatives (RD 01-12) were designed, synthesized, and evaluated for their potential as breast cancer modulators through *in vitro*, *in silico*, and ADMET profiling. Compound RD-09 emerged as the most promising with an IC_{50} value of $1.21 \pm 0.03 \mu M$, suggesting it may act as an agonist of the epidermal growth factor receptor (EGFR), a key target in triple-negative breast cancer (TNBC). Docking studies further supported RD-09's significant potency.

KEYWORDS: Breast cancer, triazine, EGFR, Biological evaluation, triazine and thiazolidine-4-one hybrid.**1. INTRODUCTION**

Cancer is characterized by uncontrolled multiplication of cells and the ability of these cells to invade into other tissues.^[1] Cancer usually results in tumours, which are lumps of tissue caused by uncontrolled cell proliferation, with the exception of leukaemia, which impairs blood function via aberrant cell development in the bloodstream.^[2] These tumours can cause hormonal changes that impair regular body functioning and impact the neurological, circulatory, and digestive systems.^[3] Genetic alterations that interfere with the planned replacement of cells cause cancer by causing uncontrolled cell division and tumour growth^[4,5] There are several types of cancer, and each one has a unique set of distinguishing characteristics as well as a range of potential therapies.^[6] Some of the most common types of cancer include skin cancer, lung cancer, prostate cancer,

colon cancer, and breast cancer.^[7] Breast cancer is a malignant tumour that typically starts in the milk ducts of the breast. It appears when abnormal cells in the breast keep dividing and growing uncontrollably, which causes a tumour to form.^[8] With 2.3 million new cases globally in 2020, breast cancer is the most common cancer diagnosed globally.^[3] It generally starts in the milk ducts. Age, family history, certain gene variants (including BRCA1 and BRCA2), radiation exposure, hormonal variables, and lifestyle decisions like alcohol use and obesity are risk factors.^[4] Breast biopsies and MRIs are part of the diagnosis process. Treatment options include hormone treatment, targeted therapy, radiation, chemotherapy, and surgery, depending on the stage of the malignancy.^[9,10] Effective treatment and early detection are essential for survival and quality of life.^[11] In breast cancer, EGFR plays a critical role, especially in

aggressive subtypes like TNBC and IBC.^[12] An EGFR mutation or overexpression causes uncontrolled cell proliferation. Using inhibitors to target EGFR is a viable treatment strategy.^[13] EGFR inhibitors are frequently used in conjunction with chemotherapy to enhance outcomes, since they have demonstrated effectiveness in TNBC and IBC. Research continues to explore the potential of EGFR as a biomarker and therapeutic target,

aiming to enhance treatment strategies for these aggressive cancers^[14,15] the overall influence of EGFR on breast cancer demonstrated in Fig.1.1. To design novel compounds based on reported active pharmacophoric features and validate them through molecular modelling, we aimed to synthesize and characterize these designed compounds for further biological studies.

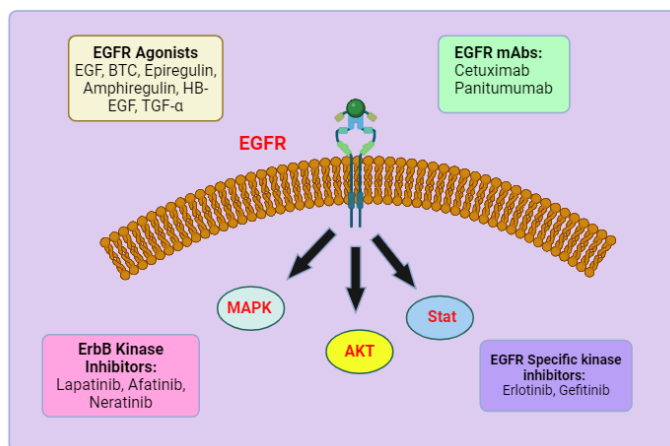


Fig. 1. 1. Overall influence of EGFR on breast cancer.

2. RESULTS AND DISCUSSIONS

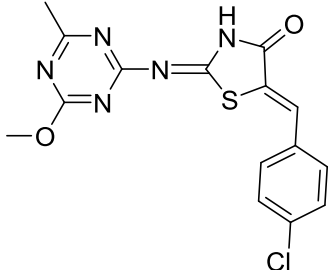
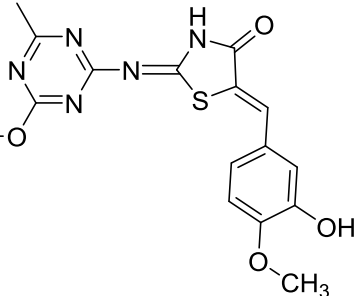
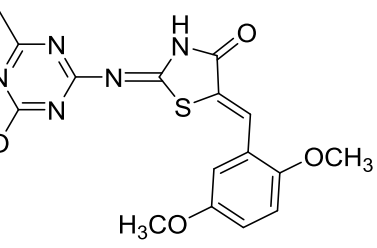
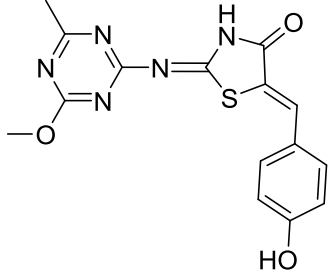
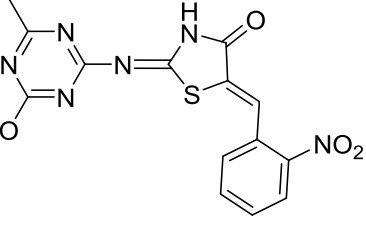
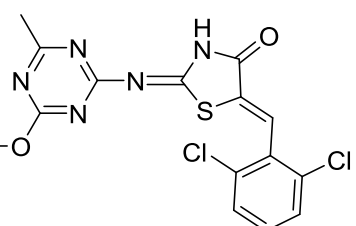
2.1. Chemistry

A series of 4-arylidene-triazinthiazolidin-4-one were prepared by reacting triazin-thiazolidin-4-one with different aromatic aldehydes as per the protocol shown in synthetic scheme. The formation of 4-arylidene-triazinthiazolidin-4-one was confirmed by the appearance of a characteristic proton signal around δ 9.74 ppm, along

with the aromatic signals in ¹HNMR. ¹HNMR, ¹³CNMR spectral analysis of all the synthesised compounds agree with the reported value. For 4-arylidene-triazinthiazolidin-4-one derivatives, characteristic bands in the IR were noticed at 1680–1670 for the carbonyl group (C=O), 1680–1640 for the carbonyl group (C=C). All the synthesised compounds are depicted in Table 2.1.

Table 2.1: Physicochemical parameters of the final compounds (RD01-RD12)

Code (1-12)	Structure	Reaction Time	Melting Point (°C)	Appearance	Yield (%)	Solvent system
RD-01		8 hr	168-170	Yellow	72	Hexane: Acetone 7: 3 R _f value: 0.6 R ₁ spot: Int (e ₂) R ₂ spot: p-methoxy benzaldehyde Co spot: R ₁ , R ₂ , P P spot: Product
RD-02		7 hr	164-166	Orange	80	Hexane: Ethyl acetate 7: 3 R _f value: 0.68 R ₁ spot: Int (e ₂) R ₂ spot: p-dimethyl amino benzaldehyde Co spot: R ₁ , R ₂ , P P spot: Product

RD-03		8 hr	154-156	Dark Yellow	63	Hexane: Ethyl acetate 7: 3 R _f value: 0.63 R ₁ spot: Int (e ₂) R ₂ spot: p-chloro benzaldehyde Co spot: R ₁ , R ₂ , P P spot: Product
RD-04		9 hr	162-164	Dark Brown	75	Hexane: Acetone 7: 3 R _f value: 0.67 R ₁ spot: Int (e ₂) R ₂ spot: isovanillin Co spot: R ₁ , R ₂ , P P spot: Product
RD-05		7 hr	166-168	Yellow	72	Hexane: Ethyl acetate 8 : 2 R _f value: 0.52 R ₁ spot: Int (e ₂) R ₂ spot: 2,5-dimethoxy benzaldehyde Co spot: R ₁ , R ₂ , P P spot: Product
RD-06		8 hr	156-158	Dark Brown	65	Hexane: Ethyl acetate 7: 3 R _f value: 0.63 R ₁ spot: Int (e ₂) R ₂ spot: 2-nitro benzaldehyde. Co spot: R ₁ , R ₂ , P P spot: Product
RD-07		10 hr	167-169	Yellow	74	Hexane: Ethyl acetate 8: 2 R _f value: 0.68 R ₁ spot: Int (e ₂) R ₂ spot: 2,5-dichloro benzaldehyde Co spot: R ₁ , R ₂ , P P spot: Product
RD-08		9 hr	161-163	Brown	60	Hexane: Acetone 7: 3 R _f value: 0.71 R ₁ spot: Int (e ₂) R ₂ spot: 2,5-dihydroxy benzaldehyde Co spot: R ₁ , R ₂ , P P spot: Product

RD-09		10 hr	164-166	Dark Brown	78	Hexane: Ethyl acetate 7: 3 R _f value: 0.65 R ₁ spot: Int (e ₂) R ₂ spot: 2,3,4-tri hydroxy benzaldehyde Co spot: R ₁ , R ₂ , P P spot: Product
RD-10		9 hr	169-171	Orange	62	Hexane: Ethyl acetate 7: 3 R _f value: 0.64 R ₁ spot: Int (e ₂) R ₂ spot: 2,3,4-trimethoxy benzaldehyde Co spot: R ₁ , R ₂ , P P spot: Product
RD-11		8 hr	178-180	White	68	Hexane: Ethyl acetate 7: 3 R _f value: 0.71 R ₁ spot: Int (e ₂) R ₂ spot: 2,3,4-trimethoxy benzaldehyde Co spot: R ₁ , R ₂ , P P spot: Product
RD-12		8 hr	168-170	Black	61	Hexane: Ethyl acetate 7: 3 R _f value: 0.64 R ₁ spot: Int (e ₂) R ₂ spot: 2,3,4-trimethoxy benzaldehyde Co spot: R ₁ , R ₂ , P P spot: Product

2.2. In-silico activity

Molecular docking studies

Based on literature, 30 compounds were designed and screened against the EGFR target. Out of these 30 compounds, 12 compounds demonstrated significantly higher docking scores compared to the others. These 12 compounds were subsequently synthesized. The Molecular docking studies of the synthesised compounds were performed against EGFR enzyme (PDB ID: 5UGA) using GLIDE module of Schrodinger 9.4. The compound, RD-09 showed the highest binding energy with values of -7.302 kcal/mol. The docking score of the potent compound along with their interaction have been presented in Table 5.2. The docking protocol was validated by extracting the ligand and superimposed over the standard ligand Erlotinib in the active pocket of

EGFR and the RMSD value was found to be negligible. The synthesized compound RD-09 get completely accommodated in the binding pocket of EGFR, followed the same pattern as the reference and displayed a docking score comparable of Erlotinib (-5.758 kcal/mol). THR854, GLN791 are the prominent amino acids involved in the interaction of RD-09 with the active site of EGFR. From this we can conclude that most of the synthesised compounds have a higher docking score as compared to the standard Erlotinib among which RD-09 have the highest docking score thus making it the most desirable compound. The binding patterns of the potent compound RD-09 and Erlotinib is given in Fig. 2.1, Fig. 2.2, Fig. 2.3, Fig. 2.4, which also represents their 2D and 3D interaction.

Table 2.2: Molecular docking of the synthesised compounds against PDB ID- 5UGA

Sl. No	Compound	Docking Score
1	RD-01	-5.802
2	RD-02	-7.05
3	RD-03	-6.764

4	RD-04	-5.951
5	RD-05	-4.986
6	RD-06	-7.299
7	RD-07	-6.47
8	RD-08	-6.6
9	RD-09	-7.302
10	RD-10	-3.977
11	RD-11	-7.299
12	RD-12	-6.537
	Erlotinib	Standard
		-5.758

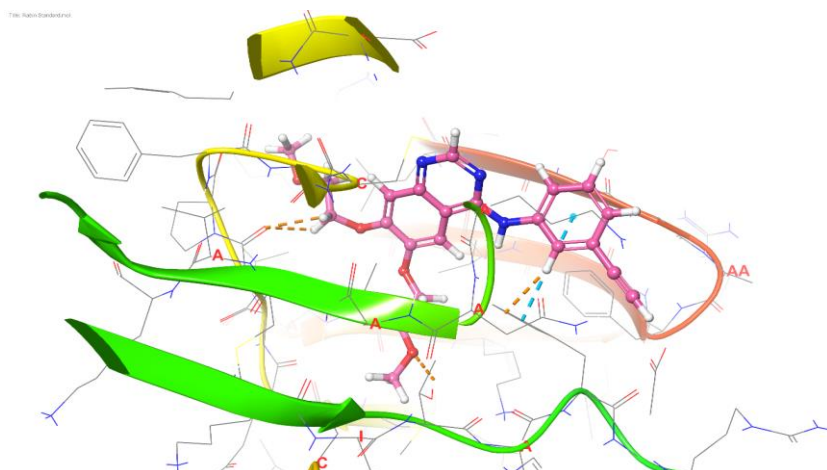


Fig. 2.1. 3D representation of Erlotinib (standard) on the active site of EGFR (PDB ID: 5UGA).

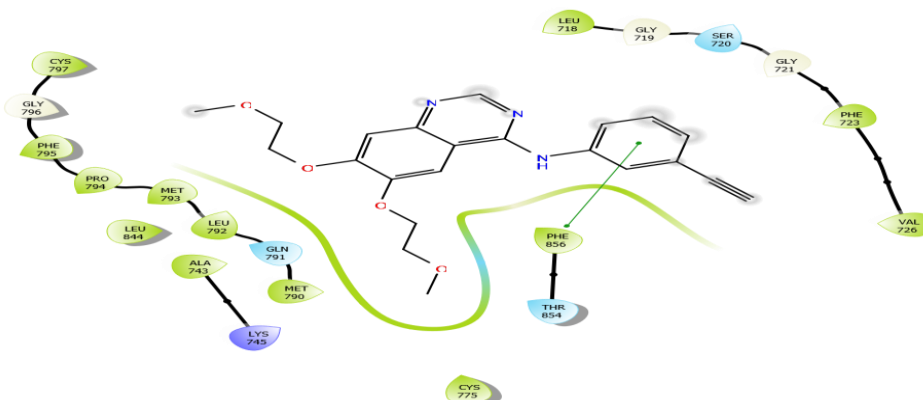


Fig. 2.2. 2D representation of Erlotinib (standard) on the active site of EGFR (PDB ID: 5UGA).

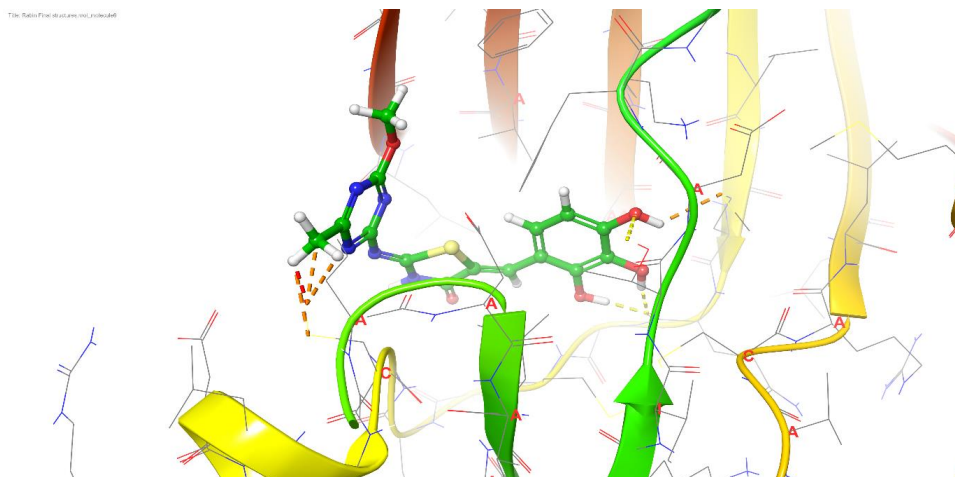


Fig.2.3. 3D representation of RD-9 on the active site of EGFR (PDB ID: 5UGA).

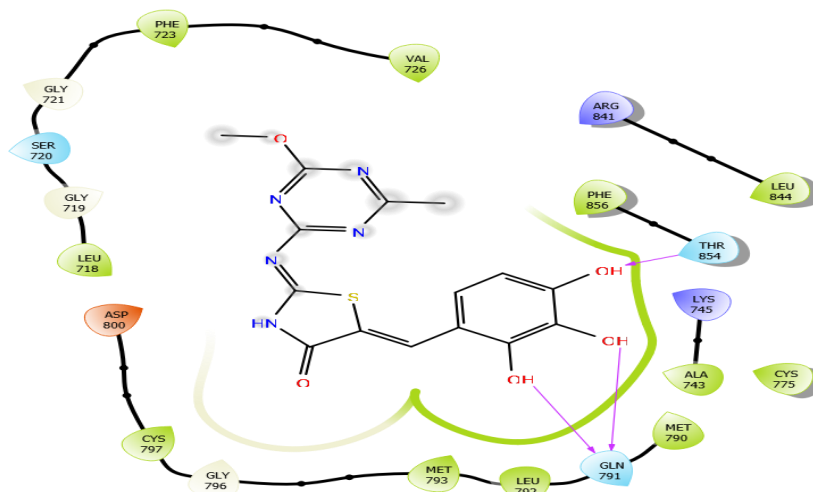


Fig. 2.4. 2D representation of RD-9 on the active site of EGFR (PDB ID: 5UGA).

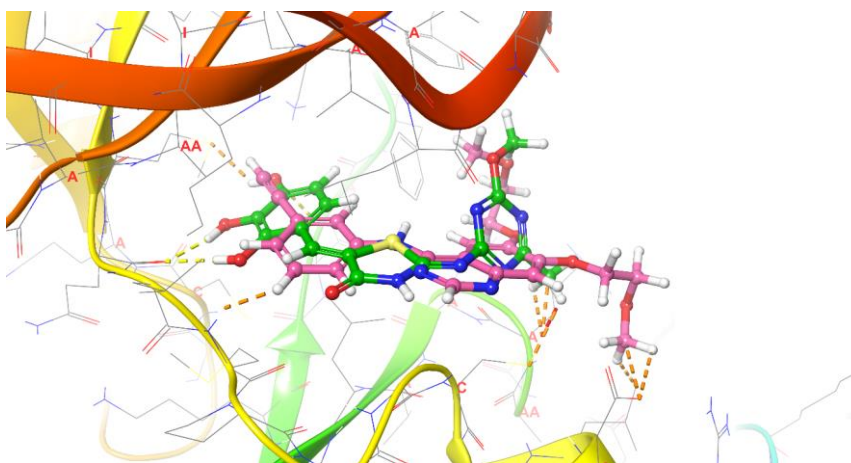


Fig. 2.5. Superimposition of Erlotinib (Standard) and RD-09 on the active site of EGFR (PDB ID: 5UGA).

2.3. *In-silico* ADME property

In order to predict the ADME studies of the synthesized compounds online free software Swiss ADME was used (<http://www.swissadme.ch/>). The ADME studies were shown in Table 2.4. The result revealed that no

synthesized compound violated the Lipinski rule of five and had great oral bioavailability. All predicted parameters were within the recommended range and no compound showed toxicity.

Table 5.4: ADME properties of the synthesised compounds.

Compounds	MW	Rotatable bonds	H-bond acceptors	H-bond donors	TPSA (\AA^2)	Log P	GI absorption	Lipinski violations
RD-1	357.39	4	7	1	123.89	3.29	High	0
RD-2	370.43	4	6	1	117.90	3.19	High	0
RD-3	361.81	3	6	1	114.66	3.23	High	0
RD-4	373.39	4	8	2	144.12	3.11	High	0
RD-5	387.41	5	8	1	133.12	3.54	High	0
RD-6	372.36	4	8	1	160.48	2.57	High	0
RD-7	396.25	3	6	1	114.66	3.29	High	0
RD-8	359.36	3	8	3	155.12	2.21	High	0
RD-9	375.36	3	9	4	115.82	2.93	High	0
RD-10	417.44	6	9	1	142.35	3.61	High	0
RD-11	372.36	4	8	1	160.48	2.65	High	0
RD-12	372.36	4	8	1	160.48	2.60	High	0
Erlotinib	393.44	10	6	1	74.73	3.67	High	0

MW= molecular weights, RB= rotatable bonds, HBA- hydrogen bond acceptors, HBD= hydrogen bond donor, TPSA= total polar surface area, GI absorption= Gastrointestinal absorption.

2.4. *In-vitro* activity

Table 2.3: *In vitro* EGFR inhibitory activity for compounds RD (01-12) and Erlotinib.

Sl. No	IC ₅₀ (mean ± SEM) (μM)	
	Compound	EGFR
1	RD-01	15.03 ± 0.02
2	RD-02	10.29 ± 0.06
3	RD-03	8.33 ± 0.18
4	RD-04	16.43 ± 0.25
5	RD-05	17.09 ± 0.05
6	RD-06	13.22 ± 0.13
7	RD-07	7.16 ± 0.15
8	RD-08	5.23 ± 0.22
9	RD-09	2.21 ± 0.03
10	RD-10	13.25 ± 0.05
11	RD-11	12.54 ± 0.28
12	RD-12	12.91 ± 0.11
13	Erlotinib	1.38 ± 0.05

The concentration of test compound produces 50% inhibition EGFR enzyme, the result is obtained by the Kinase-Glo Plus luminescence kinase assay kit³². The *in vitro* EGFR inhibitory activity for compounds RD (01-12) and Erlotinib was evaluated using the Kinase-Glo Plus luminescence kinase assay kit. All the synthesised compounds demonstrated 50% inhibition against the EGFR enzyme. Among the synthesised compounds, compound RD-09 showed the most potent activity, with

an IC₅₀ value of 2.21 ± 0.03 μM, which was similar effective with the standard Erlotinib, which had an IC₅₀ value of 1.38 ± 0.05 μM. This finding was also supported by docking studies, which indicated that RD-09 was the most potent among all synthesised compounds, surpassing the standard Erlotinib. Given below is the graphical representation of the activity of the compounds along with the standards in Fig. 2.6.

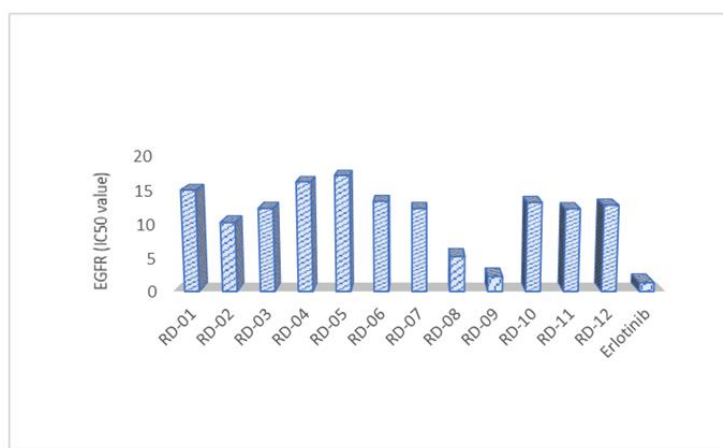


Fig. 2.6. The graphical representation of the activity of the compounds along with the standards.

2.3.1. Structure-activity relationship (SAR) analysis

The structure-activity relationship (SAR) of the synthesised compound indicates that the allylic bond is essential for its anticancer activity, and removing this bond results in decreased activity. Furthermore, when the

R group is present in the phenyl ring of substituted aldehydes, several trends are observed. Electron-withdrawing groups, such as Cl or NO₂, positioned in the para position, enhance the activity compared to electron-donating groups. Additionally, substituting the ortho,

meta, or para positions with an OH group leads to the most potent activity, with the para position mono-substituted OH group specifically increasing the activity.

In contrast, substituents such as OCH₃ decrease the activity, whereas dichloro substitution leads to an increase in activity.

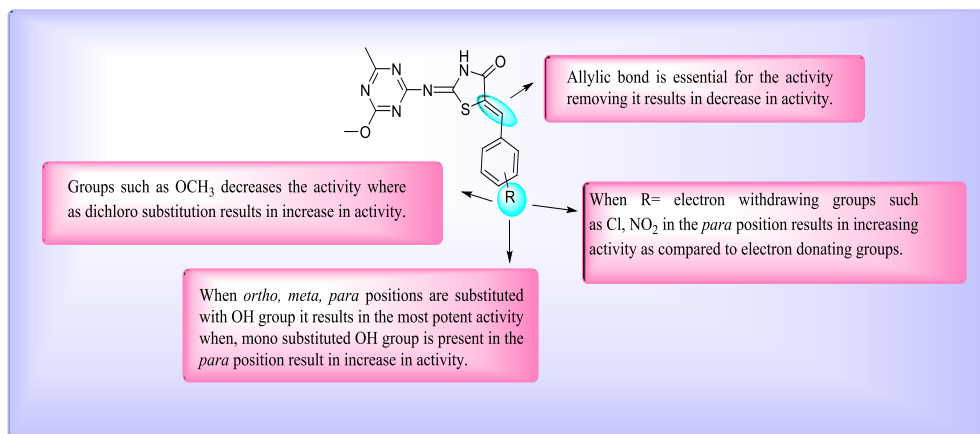


Fig. 2.7. Structure-activity relationship (SAR) of the synthesised compounds.

3. MATERIALS AND METHODS

3.1. Chemistry

Oven-dried glassware and dry, pure solvents were used in the tests. The majority of the chemicals came from Avra, TCI and Sigma-Aldrich. The synthesis employed only laboratory and analytical reagent grade ingredients. Thin-layer chromatography (TLC) on pre-coated silica plates (Merck Silicagel F254) was used to monitor the reaction. A solvent system consisting of hexane, ethyl acetate, methanol, hexane, and chloroform-methanol was used. By using ultraviolet (UV) light at 254 nm or iodine vapour to see the reactants and products, the purity of each was determined. Ethanol was used to recrystallize the compounds. Using a melting point device, the compounds' melting points were found. Using potassium bromide pellets and a Thermo-Scientific FT-IR spectrophotometer, infrared (IR) spectra were captured and uncorrected. Nuclear magnetic resonance (¹H-NMR) and carbon-13 nuclear magnetic resonance (¹³C-NMR) spectra of the synthesised compounds were recorded using CDCl₃ as solvent. Parts per million (ppm) was the unit of measurement for chemical shifts with respect to the internal standard tetramethylsilane (TMS), whereas

coupling constant (J) values were expressed in Hertz (Hz). Data from mass spectrometry were acquired by the use of liquid chromatography-mass spectrometry (LCMS).

3.2. Synthetic procedure of 5-((Z)-(substituted) benzylidene)-2-((4-methoxy-6-methyl-1,3,5-triazin-2-yl) imino) thiazolidin-4-one.

3.2.1. Synthesis of 2-chloro-N-(4-methoxy-6-methyl-1, 3, 5-triazin-2-yl) acetamide (c_1)

A 0.5g (0.003 mol) sample of 4-methoxy-6-methyl-1, 3, 5-triazin-2-amine (a) was mixed dropwise with 0.01 mol of chloroacetyl chloride (b) under anhydrous conditions at 0–5°C for 6 hours. The TLC was run in the solvent system comprising of ethyl acetate and n-hexane at a ratio of 3:7. After TLC confirmation, ice cubes and sodium bicarbonate (NaHCO₃) were used for the workup. NaHCO₃ was chosen because it neutralises excess chloroacetyl chloride, which leads to the development of vigorous effervescence. Filtration was done using Whatman filter paper, the reaction mixture was filtered out under vacuum using a vacuum pump and the compound was recovered and dried.

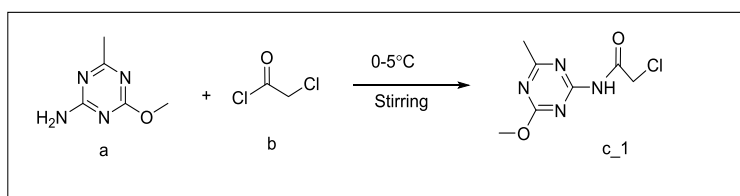


Fig. 3.1. Synthesis of 2-chloro-N-(4-methoxy-6-methyl-1,3,5-triazin-2-yl)acetamide (c_1).

3.2.2. Synthesis of 2-((4-methoxy-6-methyl-1, 3, 5-triazin-2-yl) imino) thiazolidin-4-one (e_2)

The synthesis of thiazolidin-4-one involved dissolving 0.5g (0.002 mol) of substituted acetamide (c_1) in ethanol using a magnetic stirrer, after which 0.35g (0.004 mol) of ammonium thiocyanate (d) was added to the mixture, and heated in an oil bath at 90-100 °C for 8 h.

TLC was used to monitor the progression of the reaction in the solvent system comprising of acetone and n-hexane having a ratio of 2:8. Upon TLC confirmation, workup was done using ice cubes, the product (e_2) was then filtered using Whatman filter paper under vacuum by the aid of a vacuum filter.

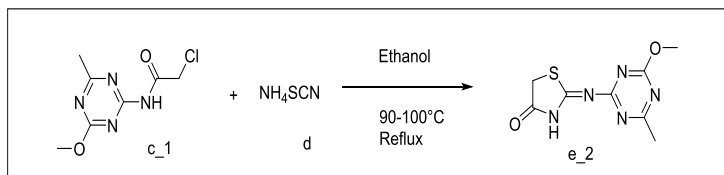


Fig. 3.2. Synthesis of 2-((4-methoxy-6-methyl-1,3,5-triazin-2-yl)imino)thiazolidin-4-one (e₂).

3.2.3. General Procedure for the synthesis of 5-((Z)-(substituted) benzylidene)-2-((4-methoxy-6-methyl-1,3,5-triazin-2-yl) imino) thiazolidin-4-one (RD01-RD12)

To the solution of 0.2g (0.002 mol) (e₂) in 3 ml of ethanol substituted aldehyde (f) was added and 3-5 drops of piperidine was also added and the reaction was refluxed and continuously stirred and heated in an oil bath at 90-100°C using a magnetic stirrer for 7-8 hours resulting in the formation of the compound (g). The progress of the reactions was observed by using TLC. Upon TLC confirmation, the workup was carried by using ice cubes and the compound was filtered by using Whatman filter paper and recrystallised using ethanol.

5-((Z)-4-(dimethylamino)benzylidene)-2-((4-methoxy-6-methyl-1,3,5-triazin-2-yl)imino)thiazolidin-4-one (RD-02), Solid, Orange, Melting point- 164-166 °C, IR (KBr, cm⁻¹): 3453.98 (N-H), 1661.00 (C=O), 1601.00 (aliphatic

C=C), 3453.98 (N-H), 1481.95 (aromatic C=C), 1345.53 (C-N), ¹H NMR (500 MHz, CDCl₃, δ ppm): δ: 9.74(s, 1H, NH), 7.74 (s, 1H, CH), 7.26(d, 1H, 2'', 6''), 6.71(d, 1H, 3'', 5''), 4.00(s, 3H, CH₃), 3.06(s, 3H, CH₃), 2.49(s, 1H, 6), ¹³C NMR (125 MHz, CDCl₃, δ ppm): δ: 190.33; 154.36; 131.99; 125.22; 111.02; 77.28; 76.77; 40.09, LCMS (M-H):369.16(base peak, 100%)

2-((4-methoxy-6-methyl-1,3,5-triazin-2-yl)imino)-5-((Z)-2,3,4-trihydroxybenzylidene)thiazolidin-4-one (RD-09), Solid, Dark brown, Melting point- 164-166°C, IR (KBr, cm⁻¹): 3324.60 (N-H), 1680.52 (C=O), 1660.20 (aliphatic C=C), 3143.95 (O-H), 1462.75 (aromatic C=C), ¹H NMR (500 MHz, CDCl₃, δ ppm): δ: 9.74(s, 1H, NH), 7.33 (s, 1H, OH), 7.33(s, 1H), 7.34(s, 1H, OH), 7.15(d, 1H, 6''), 6.95(d, 1H, 5'), 7.14(s, 1H, CH), 3.09(s, 3H, CH₃), 2.53(s, 3H, CH₃), ¹³C NMR (500 MHz, CDCl₃, δ ppm): δ: 189.59; 156.74; 153.63; 124.97; 123.51; 113.38; 110.45; 77.28; 77.02, 76.77, 56.19, 55.03, LCMS (M-H):375.71(base peak, 100%)

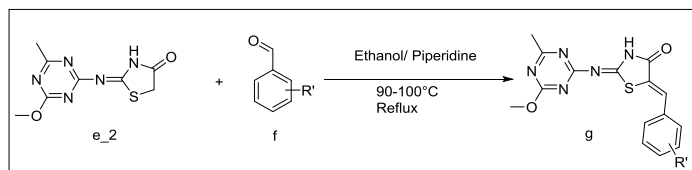


Fig. 3.3. Synthesis of 5-((Z)-(substituted) benzylidene)-2-((4-methoxy-6-methyl-1,3,5-triazin-2-yl) imino) thiazolidin-4-one (RD01- RD12).

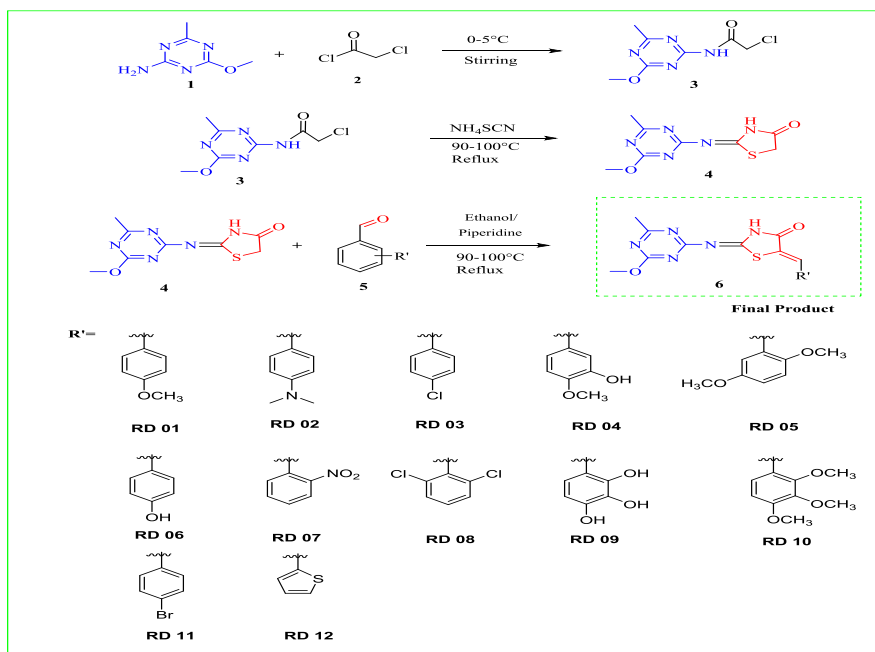


Fig. 3.4. Synthetic scheme Synthesis of 5-((Z)-(substituted) benzylidene)-2-((4-methoxy-6-methyl-1,3,5-triazin-2-yl) imino) thiazolidin-4-one (RD01- RD12).

3.3. Biological evaluation

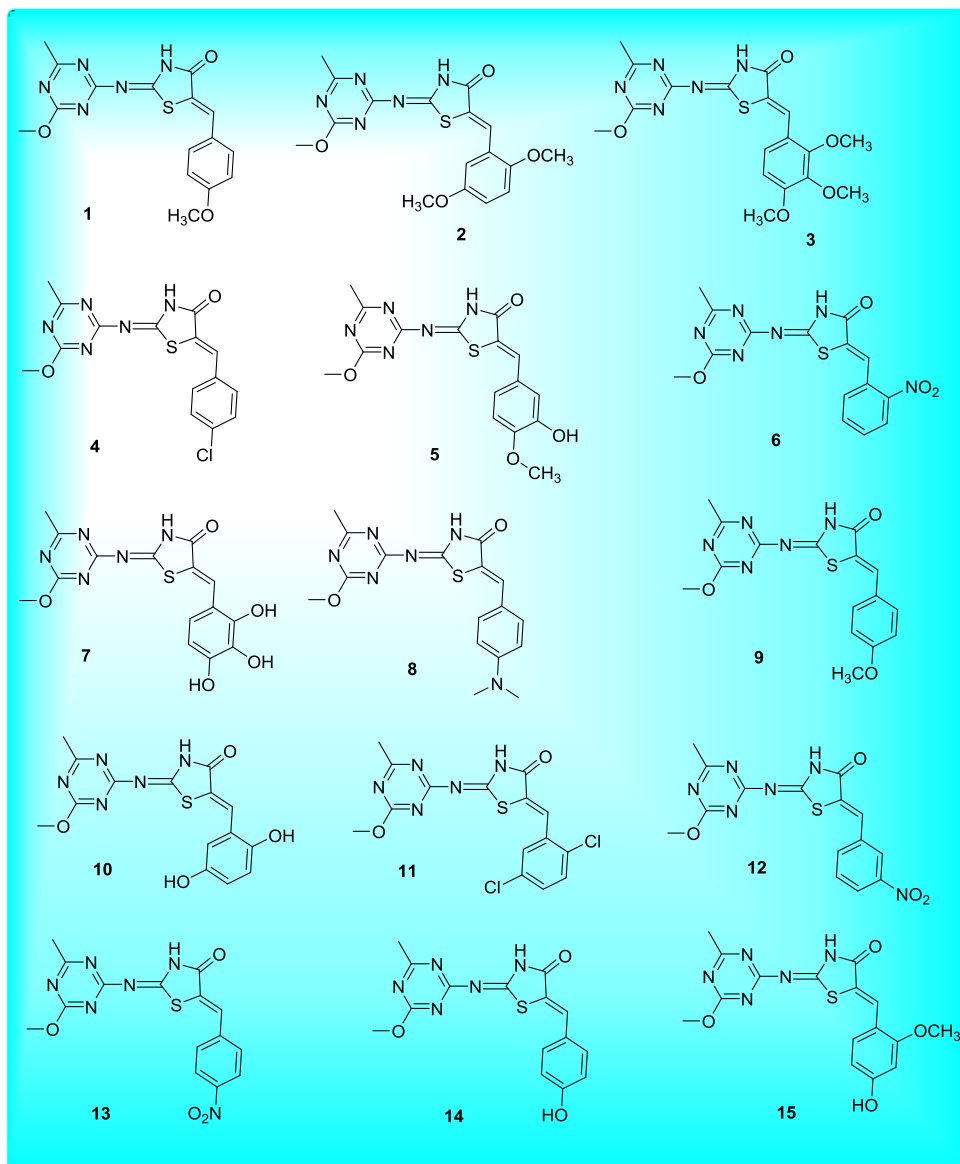
3.3.1. EGFR tyrosine kinase inhibitory activity

EGFR activity was measured by measuring the quantity of ATP left in the kinase reaction solution using the Kinase-Glo Plus luminescence kinase assay kit³². The luminescent signal is correlated with the residual amount present and it was inversely related with kinase activity. A 50 mL reaction was started with 5 mL of the 100 mM dilution of the tested chemicals in 10% DMSO. The 50 mL reaction mixture, which included 10 mM MgCl₂, 40 mM Tris, pH 7.4, 0.1 mg/mL BSA, 0.2 mg/mL Poly (Glu, Tyr) substrate, 10 mM ATP, and EGFR, was used for all of the enzymatic reactions, which were carried out at 30 °C for 40 minutes. For each response, add 50 mL of the Kinase-GloPlus Luminescence Kinase Assay after incubating the plate for five minutes at room temperature. The protein kinase test kit known as ADP-Glo is used to measure ADP production, which increases luminescence signal and is used to estimate IC₅₀ values. The test was incubated by adding 25 mL of ADP-Glo reagent to the reaction mixture after it had been

incubated for 30 minutes at 30 °C in a 96-well plate. After 30 minutes of shaking at room temperature, the 96-well plate is incubated, and 50 mL of kinase detection reagent is added. Utilising the ADP-Glo Luminescence reader, read the 96-well plate. With the exception of the substrate, every assay component was introduced to the blank control. The adjusted activity for every protein kinase target may be obtained by subtracting the blank control value.

3.4. *In silico* studies

Initially, 30 compounds were designed using various substituted aldehydes and drawn using ChemDraw Professional 16.0 software. These compounds were docked against the EGFR receptor to evaluate their potential efficacy. Based on their docking scores, 12 compounds showing higher potency were selected for synthesis. This selection process ensured that only the most promising candidates, as indicated by their superior docking scores, were chosen for further synthesis and named as RD (01-12) series.



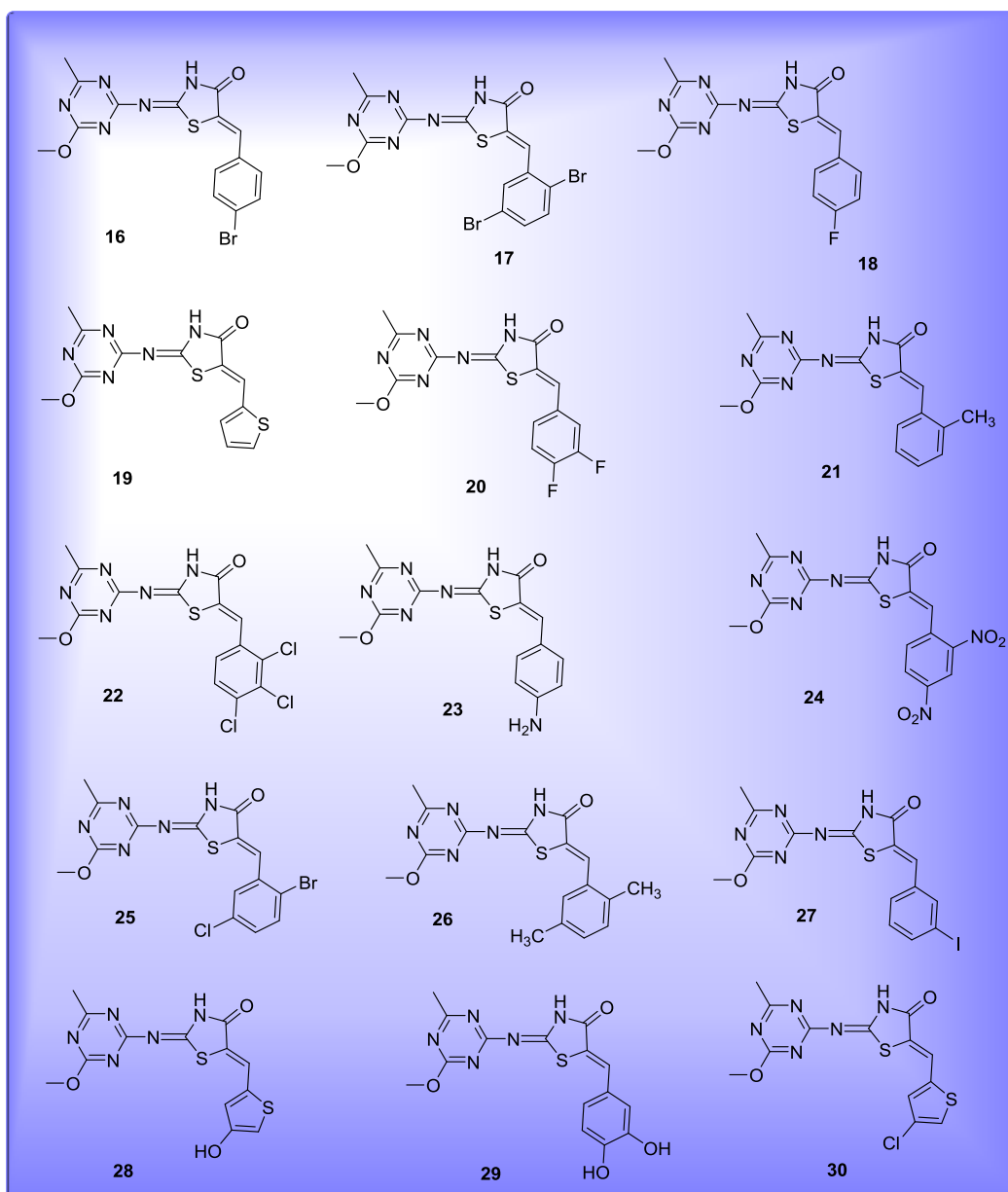


Fig. 3.5. Different compounds that were designed.

3.4.1. Protein and ligand preparation

The crystal structures (PDB ID: 5UGA) of EGFR were prepared using the Prep wizard of the Maestro software package. After addition of hydrogen atoms, bond orders and formal charges were checked, following which minimization was performed. The ligands were prepared using the LigPrep tool (Maestro 9.6).

3.4.2. Molecular Docking

Using Schrödinger 9.6 Maestro version software, molecular docking studies for newly synthesized derivatives RD (01-12) were carried out at the molecular level in the EGFR kinase receptor (PDB ID: 5UGA) in order to understand the binding mode of these compounds. By the application of LigPrep tool (Maestro 9.6), the ligands were prepared for docking, and in the 3D format, they were sketched by the build panel, the protein for the docking study was taken and prepared

using the protein preparation wizard (pepwizard) by adding hydrogen further energy minimization was done. The synthesised compounds and co-crystallized ligand Erlotinib were then docked using the GLIDE module of Schrodinger 9.4 against binding site of EGFR.

3.5. *In silico* ADME Properties

The various structural and physicochemical parameters of the synthesised molecules influence the molecule's drug-likeness. Predicting the drugs' oral bioavailability is helpful. That is, the chemical must abide by Lipinski's five rules in order to be drug-like or not to function as a therapeutic molecule. The five rules of Lipinski's rule of five are as follows: (a) the number of hydrogen bond donors should not be more than 5, (b) the number of hydrogen bond acceptors should not be more than 10, (c) Molecular mass should be less than 500 Daltons, (d) log P (octanol- water partition coefficient) should not be

greater than 5. In the present study, the drug-likeness characteristic of the compound was calculated with the aid of the online tool Swiss ADME tools.

CONCLUSION

In this study, triazine-4-thiazolidinone derivatives were designed, synthesized, and evaluated using *in vitro*, *in silico*, and ADMET profiling to identify potential modulators of breast cancer. Among the series of twelve new derivatives (RD 01-12), compound RD-09 emerged as the most promising, demonstrating significant potency with an IC₅₀ value of 1.21 ± 0.03 μM. This was further confirmed by docking studies, suggesting that RD-09 may act as an agonist of the epidermal growth factor receptor (EGFR), a crucial target in the treatment of triple-negative breast cancer (TNBC). The extensive characterization of these compounds using IR, NMR, and mass spectrometry underscored the robust structural integrity and biological activity of RD-09. The EGFR activity assays indicated that RD-09 was the most effective compound among those tested, exhibiting excellent *in vitro* and *in silico* activity. The findings suggest that RD-09 could serve as a new and safer lead compound in the development of anti-cancer agents, offering a promising therapeutic approach for breast cancer, particularly for subtypes like TNBC that are difficult to treat with existing therapies. These results highlight the potential of triazine-4-thiazolidinone hybrids in breast cancer treatment.

ACKNOWLEDGEMENT

I would like to express my gratitude to ISF College of Pharmacy, Moga, for their support throughout my work.

REFERENCES

- Abdu-Allah HH, Abdel-Moty SG, El-Awady R, El-Shorbagi AN. Design and synthesis of novel 5-aminosalicylate (5-ASA)-4-thiazolidinone hybrid derivatives with promising antiproliferative activity. *Bioorganic & Medicinal Chemistry Letters*, 2016 Apr 1; 26(7): 1647-50.
- Abu Samaan TM, Samec M, Liskova A, Kubatka P, Büsselberg D. Paclitaxel's mechanistic and clinical effects on breast cancer. *Biomolecules*, 2019 Nov 27; 9(12):789.
- Arnold M, Morgan E, Rungay H, Mafra A, Singh D, Laversanne M, Vignat J, Gralow JR, Cardoso F, Siesling S, Soerjomataram I. Current and future burden of breast cancer: Global statistics for 2020 and 2040. *The Breast*, 2022 Dec 1; 66: 15-23.
- Parkin DM. Global cancer statistics in the year 2000. *The lancet oncology*, 2001 Sep 1; 2(9): 533-43.
- Han SA, Kim SW. BRCA and breast cancer-related high-penetrance genes. *Translational Research in Breast Cancer*, 2021: 473-90.
- Smolarz B, Nowak AZ, Romanowicz H. Breast cancer—epidemiology, classification, pathogenesis and treatment (review of literature). *Cancers*, 2022 May 23; 14(10): 2569.
- Mavaddat N, Dorling L, Carvalho S, Allen J, Gonzalez-Neira A, Keeman R, Bolla MK, Dennis J, Wang Q, Ahearn TU, Andrulis IL. Pathology of tumors associated with pathogenic germline variants in 9 breast cancer susceptibility genes. *JAMA oncology*, 2022 Mar 1; 8(3): e216744.
- Laborda-Illanes A, Sanchez-Alcoholado L, Dominguez-Recio ME, Jimenez-Rodriguez B, Lavado R, Comino-Méndez I, Alba E, Queipo-Ortuño MI. Breast and gut microbiota action mechanisms in breast cancer pathogenesis and treatment. *Cancers*, 2020 Aug 31; 12(9): 2465.
- Li Z, Wei H, Li S, Wu P, Mao X. The role of progesterone receptors in breast cancer. *Drug design, development and therapy*, 2022 Jan 26: 305-14.
- Paplomata E, O'Regan R. The PI3K/AKT/mTOR pathway in breast cancer: targets, trials and biomarkers. *Therapeutic advances in medical oncology*, 2014 Jul; 6(4): 154-66.
- De Luca A, Maiello MR, D'Alessio A, Pergameno M, Normanno N. The RAS/RAF/MEK/ERK and the PI3K/AKT signalling pathways: role in cancer pathogenesis and implications for therapeutic approaches. *Expert opinion on therapeutic targets*, 2012 Apr 1; 16(sup2): S17-27.
- Barriga V, Kuol N, Nurgali K, Apostolopoulos V. The complex interaction between the tumor micro-environment and immune checkpoints in breast cancer. *Cancers*, 2019 Aug 19; 11(8): 1205.
- Masuda H, Zhang D, Bartholomeusz C, Doihara H, Hortobagyi GN, Ueno NT. Role of epidermal growth factor receptor in breast cancer. *Breast cancer research and treatment*, 2012 Nov; 136: 331-45.
- Thike AA, Cheok PY, Jara-Lazaro AR, Tan B, Tan P, Tan PH. Triple-negative breast cancer: clinicopathological characteristics and relationship with basal-like breast cancer. *Modern pathology*, 2010 Jan 1; 23(1): 123-33.
- Downward J, Yarden Y, Mayes E, Scrace G, Totty N, Stockwell P, Ullrich A, Schlessinger J, Waterfield MD. Close similarity of epidermal growth factor receptor and v-erb-B oncogene protein sequences. *Nature*, 1984 Feb 9; 307(5951): 521-7.